**Structural Monitoring and Maintenance**, *Vol. 4, No. 3 (2017) 237-253*
DOI: https:// doi.org/10.12989/smm.2017.4.3.237 

# Experimental investigation of magnetic-mount PZT-interface for impedance-based damage detection in steel girder connection

Joo-Young Ryu[a], Thanh-Canh Huynh[b] and Jeong-Tae Kim[*]

*Department of Ocean Engineering, Pukyong National University,*
*599-1 Daeyon-3dong, Nam-gu, Busan 608-737, Republic of Korea*

*(Received August 11, 2017, Revised September 3, 2017, Accepted September 7, 2017)*

**Abstract.** Among various structural health monitoring technologies, impedance-based damage detection has been recognized as a promising tool for diagnosing critical members of civil structures. Since the piezoelectric transducers used in the impedance-based technique should be bonded to the surface of the structure using bonding layers (e.g., epoxy layer), it is hard to maintain the as-built condition of the bonding layers and to reconfigure the devices if needed. This study presents an experimental investigation by using magnetically attached PZT-interface for the impedance-based damage detection in bolted girder connections. Firstly, the principle of the impedance-based damage detection via the PZT-interface device is outlined. Secondly, a PZT-interface attachment method in which permanent magnets are used to replace the conventional bonding layers is proposed. Finally, the use of the magnetic attraction for the PZT-interface is experimentally evaluated via detecting the bolt-loosening events in a bolted girder connection. Also, the sensitivity of impedance signatures obtained from the PZT-interface is analyzed with regard to the interface's material.

**Keywords:** magnetic-mount; electromechanical impedance; PZT interface; bolted connection; impedance-based damage detection

## 1. Introduction

In steel structures such as bridges, pipeline systems and towers, bolts are usually used to connect structural members together because of its convenience, time efficient and high reliability. The strength of the connection is guaranteed by axial internal force of bolt. However, as discontinuous parts of structures, bolted connections are influenced by severe repeated loading and various environmental conditions. These conditions may cause decrement of bolt preload or even loosening of bolt. As a result, load carrying capacity of the connection is reduced and the structure could be collapsed. Therefore, to reduce maintenance costs and to increase the reliability of structures, the structural condition of such structural connections should be accurately assessed using appropriate local structural health monitoring (SHM) techniques during their lifetime (Li *et al*. 2014, Li *et al*. 2016, Nagarajaiah *et al*. 2016, Kim *et al*. 2016).

The local SHM commonly utilizes high-frequency features to assess the integrity of local regions

*Corresponding author, Professor, E-mail: idis@pknu.ac.kr
[a] Graduate Student, E-mail: cozy1028@nate.com
[b] Post-doctoral Researcher, E-mail: ce.huynh@gmail.com


http://www.techno-press.org/?journal=smm&subpage=7 ISSN: 2288-6605 (Print), 2288-6613 (Online)

close to the sensor. By employing the high-frequency responses, the local SHM techniques can be very effective to assess the structural condition of local critical members in civil structures. Among various SHM technologies, the electromechanical (EM) impedance-based SHM has been found as an innovative and efficient approach to detect the local damage in various types of structures such as concrete structures (Soh *et al*. 2000), steel joints (Ayres *et al*. 1998, Park *et al*. 2003, Ho *et al*. 2014), pipeline systems (Park *et al*. 2003), aerospace structures (Giurgiutiu and Zagrai 2005), and tendon anchorage systems (Kim *et al*. 2010, Nguyen and Kim 2012, Huynh and Kim 2016). To detect structural changes induced by damage at critical areas, the impedance-based method employs the EM impedance responses sensed by piezoceramic patches such as PZT (i.e., lead zirconate titanate) as the local dynamic features. Liang *et al*. (1994) proposed an analytical impedance model which describes the coupling interaction between the PZT and the host structure. According to Liang's model, the impedance response measured from the PZT sensor would contain the structural information of the host structure. Therefore, the change in structural characteristics at local critical region caused by damage can lead to the variation of the impedance responses. For damage detection, the change in impedance signatures is usually quantified by the statistical pattern recognition or simply by the impedance shift at resonance (Sun *et al*. 1995, Zagrai and Giurgiutiu 2001).

In the impedance-based SHM, the sensitive frequency band of impedance signatures should be predetermined before the measurement. Generally, the sensitive frequency range is varied dependent on target structures. This causes difficulty when dealing with real structures because the sensitive frequency range is almost unknown and may take much effort to obtain it by trial and error. In order to overcome the above-mentioned limitations, a portable PZT–interface technique was proposed (Huynh and Kim 2014). The interface device is a thin-walled beam-like member with a PZT patch mounted on it. A partial free surface in the bottom of the interface is intentionally designed to make the PZT patch freely vibrating and also allow to predetermine effective frequency ranges in the impedance-based technique. The implementation of the PZT-interface was successful in indicating various tension-losses in tendon anchorage systems with sensitive frequency bands below 100 kHz (Huynh *et al*. 2015a, b).

Up-to-date, PZT interface devices used in the impedance-based SHM have been bonded to the surface of the host structure using the bonding layer such as: epoxy layer. However, the quality of the bonding layer decreases along with its service time, especially when experiencing the severe ambient condition. To ensure the accuracy of the impedance measurement and damage detection, the as-built condition of bonding layers needs to be maintained for the PZT interface devices. In addition, the attachment method via the bonding layer makes the piezoelectric devices becoming hard to be reconfigured if needed. In order to overcome the drawbacks of the conventional bonding layer, this study presents an experimental investigation into using magnetically attached PZT-interface for the impedance-based SHM. Firstly, the principle of the impedance-based damage detection via the PZT-interface device is outlined. Secondly, a PZT-interface attachment method in which permanent magnets are used to replace the conventional epoxy bond is proposed. Finally, the feasibility of using the magnetic attraction for the PZT-interface is experimentally demonstrated via detecting the bolt-loosening events in a bolted girder connection. Also, the sensitivity of impedance signatures obtained from the PZT-interface is analyzed with regard to the interface's material.

## 2. Magnetic-mount PZT-interface for impedance-based damage detection

### *2.1 Impedance-based damage detection*

To monitor structural change, a piezoelectric patch (e.g., PZT) is surface-bonded to structure at examined region, as shown in Fig. 1. The interaction between the PZT and the structure can be explained by 1-DOF free-body diagram of PZT-structure system (Liang *et al*. 1994). Due to inverse piezoelectric effect, an input harmonic voltage $V(\omega)$ induces a deformation of PZT, see Fig. 1.

Because the PZT is bonded to the structure, a force $F(\omega)$ against that deformation is induced into the host structure and the PZT as well. For 1-DOF system, the structural mechanical impedance of the host structure $Z_s(\omega)$ is obtained by the ratio of force $F(\omega)$ to velocity $\dot{u}(\omega)$ as follows (Liang *et al*. 1994)

$$Z_s(\omega) = \frac{F(\omega)}{\dot{u}(\omega)} = c + m\frac{\omega^2 - \omega_n^2}{\omega} i \tag{1}$$

where $c$ and $m$ are the damping coefficient and the mass of the structure, respectively; $\omega_n$ is the angular natural frequency of the structure; and $\omega$ is the angular frequency of the excitation voltage. As shown in Eq. (1), the structural mechanical impedance is a function of mass, damping, and stiffness (i.e., stiffness is introduced from natural frequency, $k = m\omega_n$). Thus, the change in structural parameters can be represented by the change in the structural mechanical impedance.

In the impedance-based method, the electric current I(ω) is measured from the PZT sensor and then it is utilized to calculate the overall EM impedance, as follows (Liang *et al.* 1994)

$$\mathrm{Z}(\omega) = \frac{V}{I} = \left\{ i\omega \frac{w_a l_a}{t_a} \left[ \hat{\varepsilon}_{33}^T - \frac{1}{Z_a(\omega)/Z_s(\omega)+1} d_{3x}^2 \hat{Y}_{xx}^E \right] \right\}^{-1} \tag{2}$$

where $\hat{Y}_{xx}^E = (1 + i\eta) Y_{xx}^E$ is the complex Young's modulus of the PZT patch at zero electric field; $\hat{\varepsilon}_{xx}^T = (1 - i\delta)\varepsilon_{xx}^T$ is the complex dielectric constant at zero stress; $d_{3x}$ is the piezoelectric coupling constant in x-direction at zero stress; $k = \omega\sqrt{\rho/\hat{Y}_{xx}^E}$ is the wave number where $\rho$ is the mass density of the PZT patch; and $w_a$, $l_a$, and $t_a$ are the width, length, and thickness of the piezoelectric transducer, respectively. The parameters $\eta$ and $\delta$ are structural damping loss factor and dielectric loss factor of piezoelectric material, respectively.

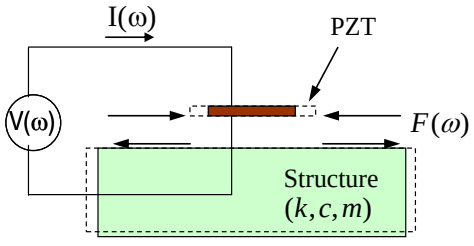


Fig. 1 Model of coupling interaction between PZT and structure

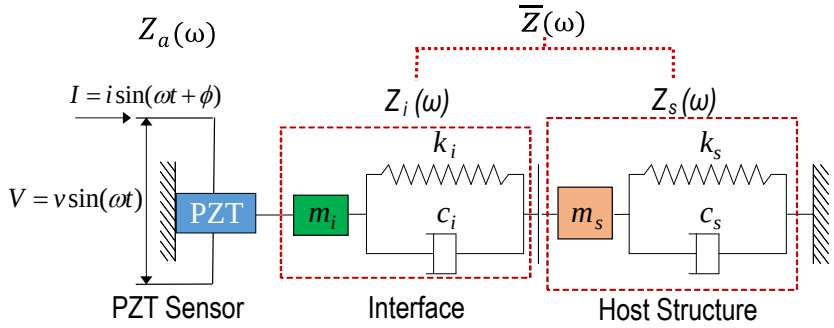


Fig. 2 Impedance model of PZT interface-host structure system (Huynh and Kim 2017)

As shown in Eq. (2), the EM impedance, $Z(\omega)$, is a combining function of the mechanical impedance of the host structure, $Z_s(\omega)$, and that of the PZT patch, $Z_a(\omega)$. The change in structural parameters ($k$, $m$, $c$) caused by damage will lead to the change in the mechanical impedance of the host structure according to Eq. (1) and result in the variation of the overall EM impedance according to Eq. (2). By this way, the damage in the host structure can be monitored via its EM impedance responses.

### *2.2 Analytical impedance model of PZT interface-host structure system*

On the basis of the previous studies (Liang *et al*. 1996, Xu and Liu 2002, Park *et al*. 2008), Huynh and Kim (2017) proposed an EM impedance model to represent coupled dynamic responses of PZT interface-host structure, as shown in Fig. 2. The PZT interface-host structure is modeled as a spring-mass-damper system, in which $m_i$, $c_i$, $k_i$ and $m_s$, $c_s$, $k_s$ are the masses, damping coefficients, and spring stiffness of the interface and the host structure generated by the PZT driving point. In this 2-DOF system, one refers to the host structure represented by the impedance $Z_s$ and the other refers to the interface represented by its impedance $Z_i$.

The SM (i.e., structural mechanical) impedance $\bar{Z}$ of the interface-host structure system at the PZT driving point is defined as the ratio between the excitation force $F_i$ and the velocity $x_i$, as follows (Huynh and Kim 2017)

$$\bar{Z} = \frac{F_i}{\dot{x}_i} = \frac{K_{11}K_{22} - (K_{12})^2}{i\omega K_{22}} \tag{3}$$

in which, the terms $[K_{ij}]$, $i,j = 1, 2$ are the dynamic stiffness of the 2-DOF system, as follows

$$\begin{bmatrix} K_{11} & K_{12} \\ K_{12} & K_{22} \end{bmatrix} = \begin{bmatrix} -\omega^2 m_i + i\omega c_i + k_i & -i\omega c_i - k_i \\ -i\omega c_i - k_i & -\omega^2 m_s + i\omega(c_i + c_s) + (k_i + k_s) \end{bmatrix} \tag{4}$$

By substituting Eq. (3) into Eq. (2), the resultant EM impedance response of the 2-DOF model of the PZT interface-host structure system can be obtained, as follows

$$\mathrm{Z}(\omega) = \left\{ i\omega \frac{w_a l_a}{t_a} \left[ \hat{\varepsilon}_{33}^T - \frac{1}{Z_a(\omega)/\bar{Z}(\omega)+1} d_{31}^2 \hat{Y}_{11}^E \right] \right\}^{-1} \tag{5}$$

The 2-DOF impedance model contains two resonant peaks in its impedance signatures which represent the two coupled vibration modes of the PZT interface-host structure system. Since the 2-

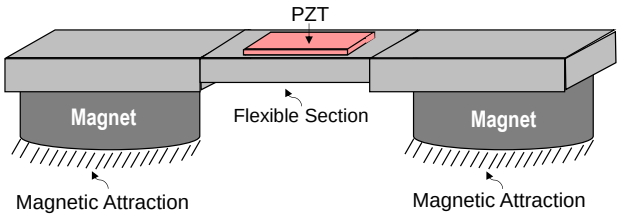


(a) Magnetic-mount PZT-interface

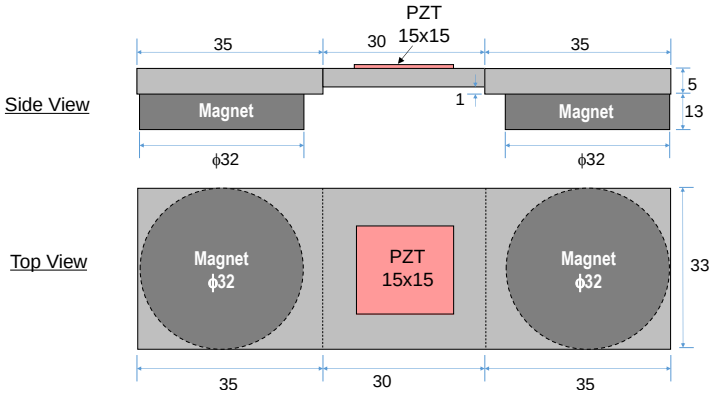


(b) Dimension (unit: mm)

Fig. 3 Prototype design of magnetic-mount PZT-interface

DOF impedance model represents the structural parameters of both the interface device and the host structure, any structural changes occurred in the host structure (or the PZT interface) can result to the changes in the measured EM impedance signatures. Therefore, the structural integrity of the host structure can be estimated by monitoring the impedance changes obtained from the PZT interface.

### *2.3 Prototype design of magnetic-mount PZT interface*

Up-to-date, PZT interface devices used in the impedance-based technique have been bonded to the surface of the structure using the bonding layer. The attachment method using the bonding layer makes the piezoelectric devices becoming hard to be reconfigured if needed. Along with its service time, the quality of the bonding layer can be also decreased, especially when experiencing the severe ambient condition. To ensure the accuracy of the impedance-based damage detection, thus, the as-built condition of bonding layers needs to be maintained for the PZT interfaces.

In order to overcome the shortcoming of the traditional bonding layers, a new attachment method via magnets was newly proposed for the PZT interface, as shown in Fig. 3. The proposed PZT interface device has a flexible beam section in the middle and the fixed-fixed boundary by two outside contact surface using permanent magnets, see Fig. 3(a). The flexible section, where the PZT sensor is installed, is intentionally designed to allow flexural vibration responses of the interface according to the piezoelectric deformation of the PZT. The two contact surfaces using permanent magnets allow the proposed interface being easily reconfigured when mounting on the surface of an

existing host structure. In addition, permanent magnets can ensure the constant adhesion performance for PZT interfaces in long-term service. These features are main advantages of the magnetic-mount PZT interface as compared to the previous interfaces.

Fig. 3(b) shows the dimensions of the magnetic-mount PZT interface, which was designed to achieve the resonant frequencies below 100 kHz for wireless impedance sensor nodes (Mascarenas *et al*. 2007, Park *et al*. 2010, Kim *et al*. 2014, Park *et al*. 2015). The proposed interface device has the following dimensions: 35x33x5 mm for the two outside bodies, 30x33x4 mm for the flexible body, $\phi$32x13 mm for the two contact magnets, and 15x15x0.51 mm for the PZT patch, see Fig. 3(b).

For the material of interface, two common metals: aluminum and steel were selected. The material properties of aluminum interface and steel interface are listed in Table 1. The magnets with gauss force of 5000 were used as the contact bodies of the interfaces. The piezoelectric properties of the PZT patch, PZT-5A, are listed in Table 2. It should be noted that the PZT sensor and magnets were bonded to the interface bodies using epoxy layers (i.e., insensitive instant adhesive Loctite 401).

## 3. Experimental evaluation of magnetic-mount PZT-interface for impedance monitoring in bolted girder connection

### *3.1 Experimental setup of bolted girder connection*

Experiments were carried out for the lab-scaled steel girder to validate the feasibility of proposed magnetic-mount PZT interface. As shown in Fig. 4(a), the test structure having a length of 4.16 m consists of two H-girders joined by two rectangular steel splice plates. 16 pairs of bolts $\phi$20 mm and nuts were used for the joint. The steel girder has the following dimensions: 200x180x8x10 mm for the cross-section of the H-girders, 310x200x10 mm for the splice plates. All bolts were fastened to 160 N.m for the intact state. A torque wrench was used to fasten the bolts and to control the bolt torques.

Table 1 Material properties of magnetic-mount interfaces

| Name | Elastic Modulus (GPa) | Mass Density ($kg/m^3$) | Magnetic Field (gauss) |
|---|---|---|---|
| Aluminum Interface | 70 | 2700 | 5000 |
| Steel Interface | 200 | 7850 | 5000 |

Table 2 Piezoelectric properties of PZT patches

| Young Modulus $Y^E_{11}$ (N/m2) | Mass Density $\rho$ (kg/m3) | Coupling Constant $d_{31}$ (m/V) | Dielectric Constant $\varepsilon^T_{33}$ (Farads/m) |
|---|---|---|---|
| 6.1x1010 | 7650 | -1.71x10-10 | 1.53x10-8 |

At the connection, two PZT interfaces were attached to the middle of the bottom splice plate, as shown in Fig. 4(b). For the performance evaluation, one PZT interface was attached to the connection using the conventional bonding layers (i.e., glue bonding interface) and other was attached using the magnetic attraction (i.e., magnetic bonding interface), as shown in Fig. 4(c). To ensure the force and strain transfer from the interface to the host structure under the PZT excitation, the splice plate was not painted and its surface was smoothened before the interface installation.

For the strain measurement, three electrical strain gauges were installed on the edges of two PZT interfaces and the middle of the splice plate, as shown in Fig. 4(c). The Kyowa data logger (EDX-100A) was used to acquire the strain signals from strain gauges and the impedance analyzer HIOKI-3532 was employed to measure the impedance signals from the PZT interfaces, as shown in Fig. 5.

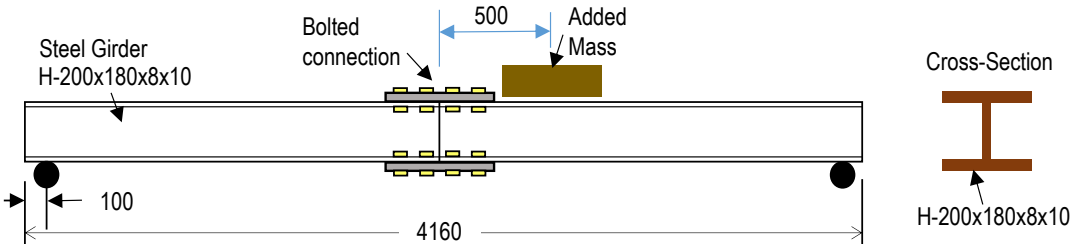


(a) Schematic of girder

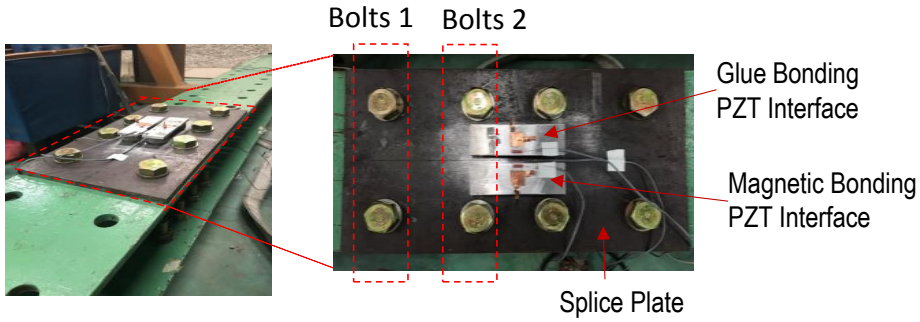


(b) Setup of bottom bolted connection

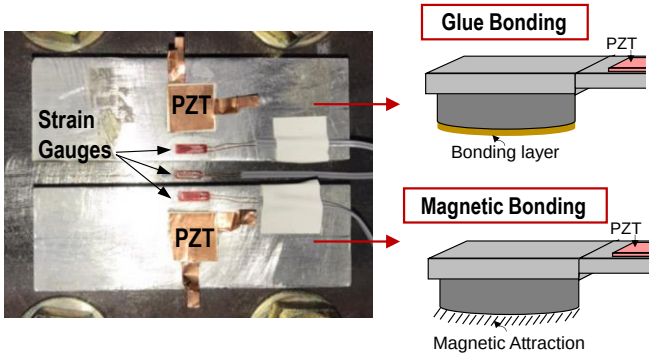


(c) Setup on PZT interfaces

Fig. 4 Experimental setup of lab-scaled steel girder connection


(a) Impedance analyser HIOKI-3532 (b) Strain data logger Kyowa EDX-100A

Fig. 5 Impedance and strain measurement system

Table 3 Added mass scenario for steel girder

| Cases | Added Mass (kN) | Cases | Added Mass (kN) |
|---|---|---|---|
| 1 | 0 | 4 | 3.6 |
| 2 | 1.2 | 5 | 4.8 |
| 3 | 2.4 | 6 | 6 |

Table 4 Bolt-loosening scenario for steel girder

| Cases | Torque-loss of Bolts 1 (%) | Cases | Torque-loss of Bolts 2 (%) |
|---|---|---|---|
| 1 | 0 | 5 | 31 |
| 2 | 31 | 6 | 62 |
| 3 | 62 | 7 | 100 |
| 4 | 100 | - | - |

Two testing scenarios were performed on the steel girder: added mass scenario and damage scenario. The added mass scenario was conducted to evaluate the bonding capability of the PZT interfaces (i.e., glue bonding and magnetic bonding interfaces) under tensile stress of the girder. The concrete blocks were sequentially loaded from 1 block (1.2 kN) to 5 blocks (6.0 kN) at a location of 50 cm from the center of the bolt connection, as shown in Fig. 4(a). For each level of the loading, strain measurements were performed for 5 minutes. Totally, six loading cases were performed as described in Table 3.

The damage scenario was carried out to evaluate the damage detectability of the PZT interfaces under bolt-loosening events in the girder connection. As the damage scenario, the bolt-loosening events of Bolts 1 and Bolts 2 were selected for the bolted connection, as indicated in Fig. 4(b). As the healthy state, all bolts were fastened to 160 N.m. To simulate damage cases, firstly, the torque of Bolts 1 was reduced by 31% (60 N.m), 62% (110 N.m) and 100% (160 N.m). Then, Bolts 1 were re-fastened. Next, Bolts 2 were loosened sequentially with the same torque-loss cases with Bolts 1. Totally, seven bolt-loosening cases were conducted for the bolted girder connection, as described in Table 4. For each level of the bolt torque, four repeated measurements of the impedance signatures were conducted. The PZT sensors were excited by a harmonic excitation voltage with 1V-amplitude,

and the impedance responses were measured in the frequency range 10-55 kHz (901 interval points).

To avoid the temperature effect, room temperature was kept within 23-24°C by air-conditioners during the tests.

### *3.2 Adhesion performance of magnetic-mount PZT interface*

#### *3.2.1 Comparison of strain responses*

The most important issue in the proposed magnetic-mount PZT interface is the adhesion performance of the magnet compared to the existing techniques that are fully attached by high-strength adhesive. When the concrete blocks were loaded at near the connection, the bottom of girder and the PZT interfaces experienced tensile deformations. Fig. 6(a) shows change of strain responses under the loading of concrete blocks for the steel girder and the two aluminum PZT interfaces (i.e., glue bonding and magnetic bonding interfaces). As observed from the figure, the strain responses at the connection were increased as the number of concrete blocks was increased. However, the strains of aluminum PZT interfaces were lower than the strain of the host structure. This result indicated that the magnetic-mount interfaces were partially attached to the connection along with the tensile deformation of the structure. For the added mass less than 4.8 kN, the magnetic attachment method provided quite consistent strain responses with the glue bonding method, see Fig. 6(a). At the added mass 6 kN, the tendency of the magnetic-based interface was not consistent with the glue bonding method. This result indicated that the magnetic-based interface was slipped on the connection under high tensile stress.

Fig. 6(b) shows change of strain responses under the loading of concrete blocks for the steel girder and the two steel PZT interfaces (i.e., glue bonding and magnetic bonding interfaces). It is observed that the strain responses at the connection were increased when increasing the number of concrete blocks. It is also observed that the strains of PZT interfaces were lower than the strain of the host structure. Along with the tensile deformation of the structure, the magnetic-mount steel interfaces were partially attached to the connection. Nonetheless, for the steel PZT interfaces, the magnetic attachment method also provided quite consistent strain responses with the glue bonding method.

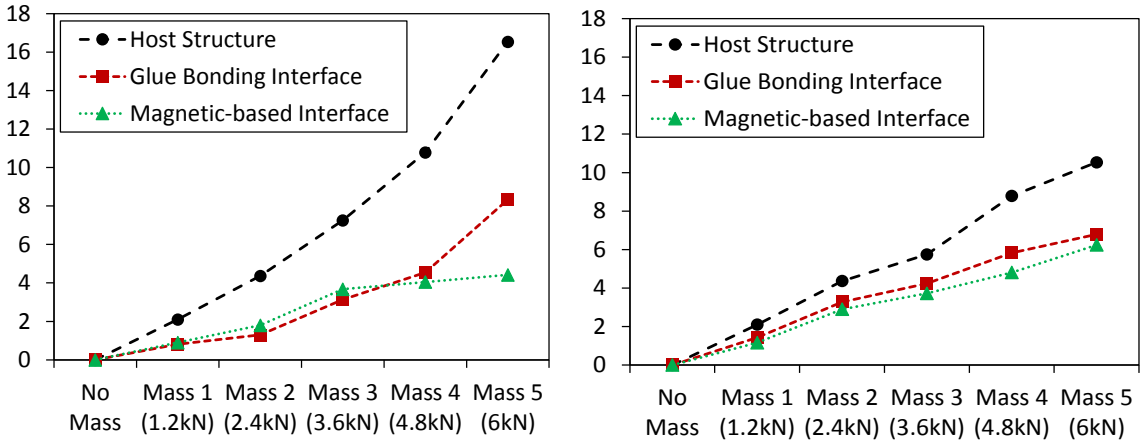


(a) Aluminum interface (b) Steel interface

Fig. 6 Strain responses of PZT interfaces and bolted connection

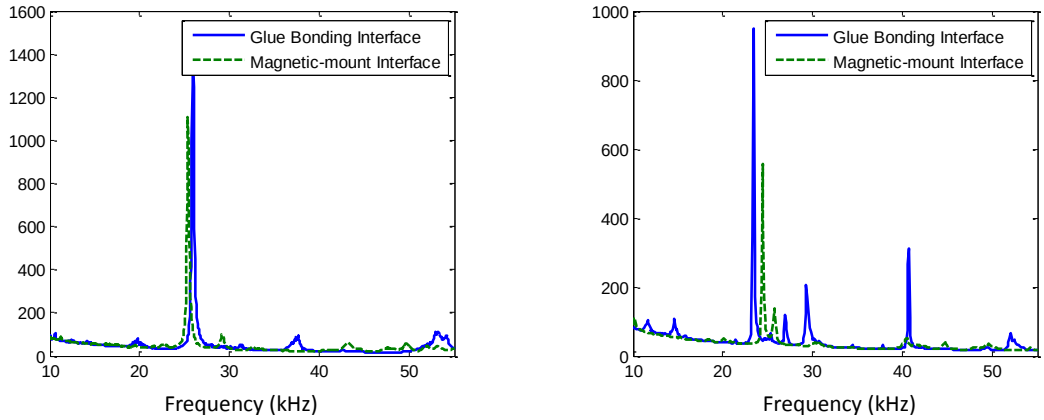


(a) Aluminum interface (b) Steel interface

Fig. 7 Comparison of impedance responses between glue bonding interface and magnetic-mount interface

By comparing Fig. 6(a) with Fig. 6(b), it is observed that when the two steel PZT interfaces were attached to the girder, the host structure experienced smaller strain variations at the pasted location of interfaces. The presence of the steel interfaces, which have higher bending stiffness than the aluminum interfaces (see Table 1), resulted in the local stiffening that reduced the strain level at the pasted location of the interfaces.

### *3.2.2 Comparison of impedance responses*

Figs. 7(a) and 7(b) show the real impedance responses of the connection in the frequency range 10 - 55 kHz under various bolt-loosening events in Bolts 1 and Bolts 2. As observed in Fig. 7(a), a few resonant peaks with different magnitudes were observed in the considered frequency range for the aluminum interfaces. It is found that the glue bonding method showed higher impedance magnitudes than the magnetic bonding method. Overall, the glue bonding method and the magnetic bonding method showed quite consistent impedance signatures at the same frequency ranges and also with identical patterns for the aluminum interfaces.

As observed in Fig. 7(b), several resonant peaks with different magnitudes were also seen in the considered frequency range for the steel interfaces. It is also observed that the glue bonding method showed higher impedance magnitudes and more resonant peaks than the magnetic bonding method. Despite those differences, the glue bonding method showed relatively similar pattern of impedance signatures with the magnetic bonding method in some frequency ranges.

## *3.3 Bolt-loosening detection performance of magnetic-mount PZT interface*

### *3.3.1 Impedance responses versus bolt-loosening events*

Figs. 8(a) and 8(b) show the real impedance signatures of the two aluminum PZT interfaces (i.e., the glue bonding and magnetic bonding methods) under the bolt-loosening events in Bolts 1 and Bolts 2. As zoomed in the figures, for the glue bonding and magnetic attachment methods, the real impedance responses were varied when the bolts were loosened. Along with the torque-loss in bolts, the model stiffness of the connection was decreased, resulting the decrement in the resonant frequencies of impedance signatures.

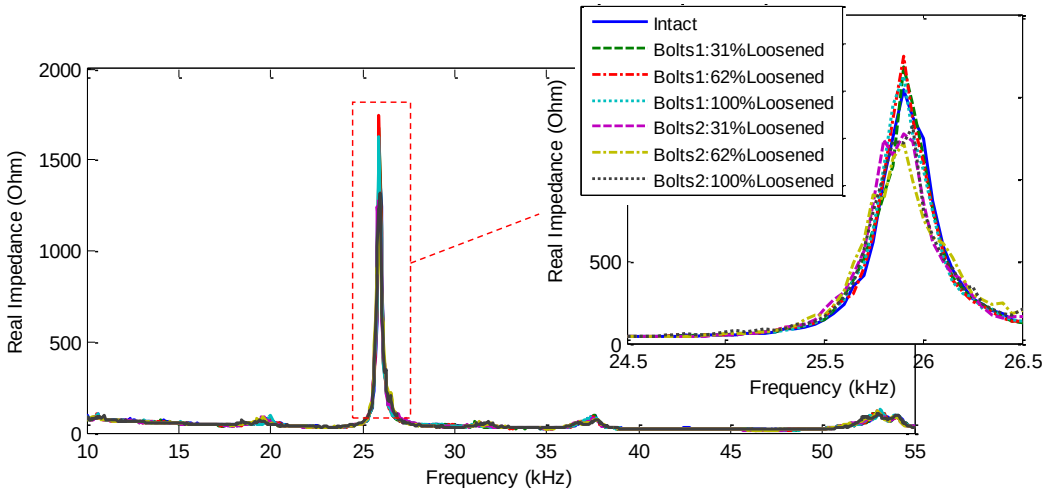


(a) Glue bonding interface

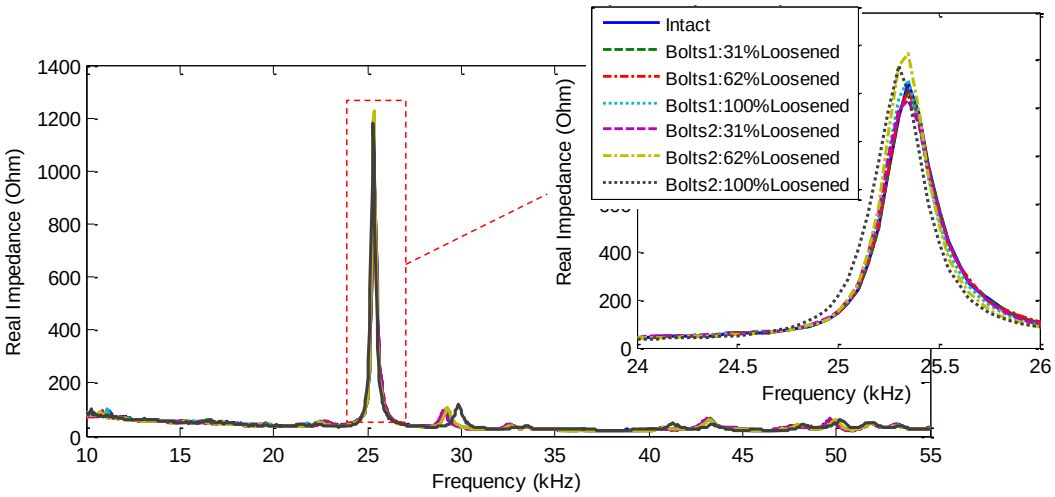


(b) Magnetic-mount interface

Fig. 8 Impedance responses of aluminum PZT interfaces under the bolt-loosening events

Figs. 9(a) and 9(b) show the real impedance signatures of the two steel PZT interfaces under the bolt-loosening events in Bolts 1 and Bolts 2. As zoomed in the figures, for the two attachment methods, the real impedance responses were sensitively varied when Bolts 1 and Bolts 2 were loosened. By comparing Fig. 9 with Fig. 8, it is found that the steel PZT interfaces showed larger variations in the impedance responses than the aluminum PZT interfaces.

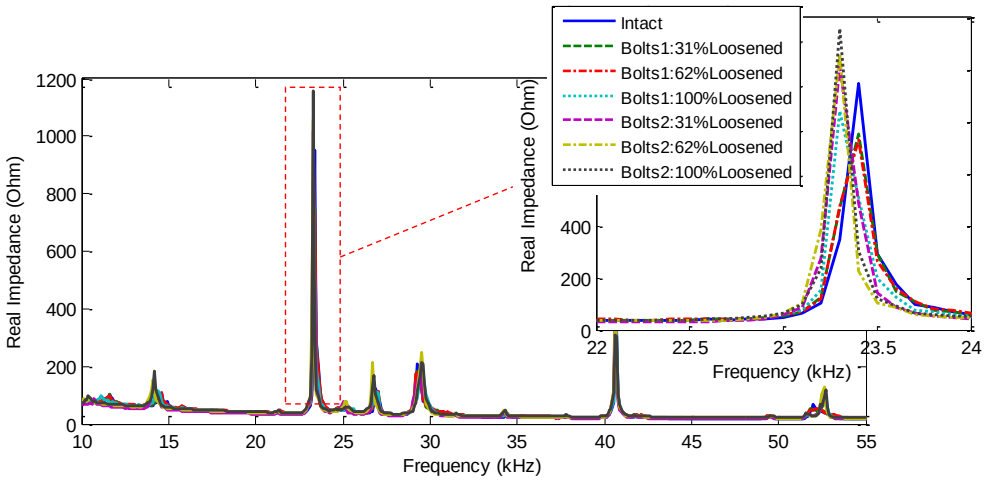


(a) Glue bonding interface

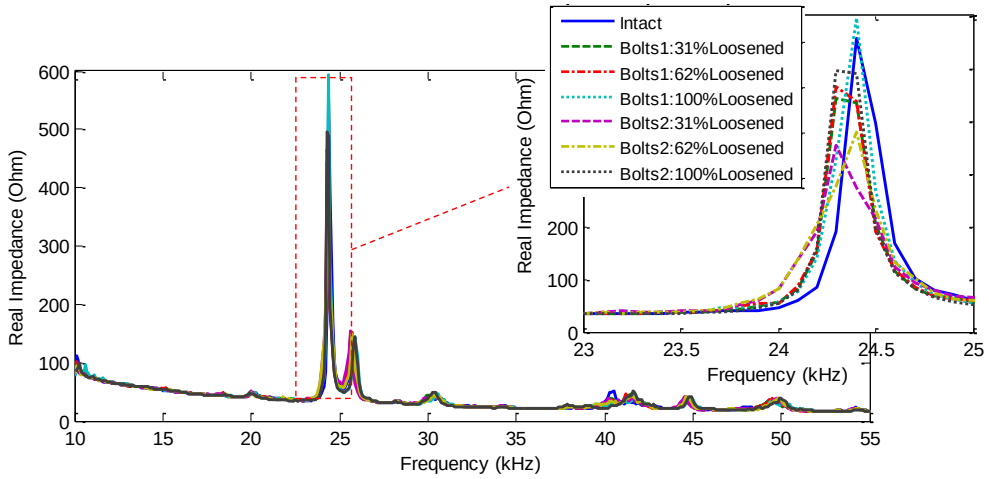


(b) Magnetic-mount interface

Fig. 9 Impedance responses of steel interfaces under the bolt-loosening events

### *3.3.2 Damage quantification by RMSD index*

To quantify the change in the EM impedance responses under the bolt-loosening events, the root mean square deviation (RMSD) index is utilized (Sun *et al*. 1995), as follows

$$RMSD(Z, Z^*) = \sqrt{\sum_{i=1}^{N}[Z^*(\omega_i) - Z(\omega_i)]^2 / \sum_{i=1}^{N}[Z(\omega_i)]^2} \quad (6)$$

where $Z(\omega_i)$ and $Z^*(\omega_i)$ are the impedances measured before and after damage for the $i^{th}$ frequency, respectively; and $N$ denotes the number of frequency points in the sweep.

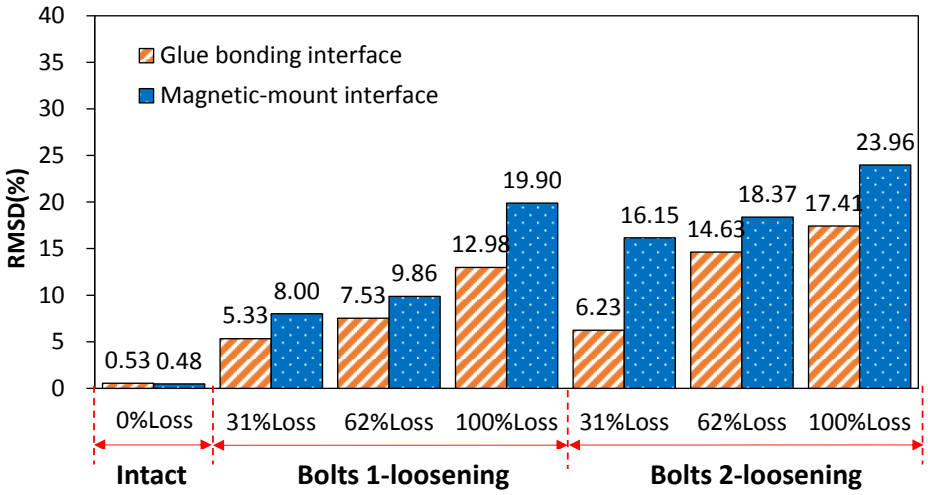


(a) Aluminum PZT interfaces

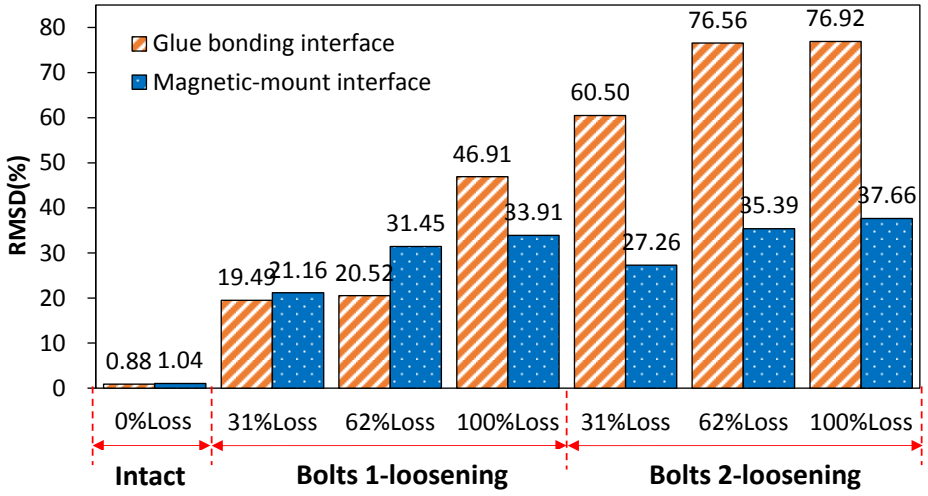


(b) Steel PZT interfaces

Fig. 10 RMSD quantification of the bolt-loosening events in steel girder

Fig.10 shows the damage quantification by RMSD index with respect to the bolt-loosening events for aluminum and steel PZT interfaces. The damage index was plotted in a row of torque-loss levels. As shown in Fig. 10(a), for the two aluminum PZT interfaces (i.e., glue bonding and magnetic bonding interfaces), the RMSD index was increased as the torque-loss in Bolts 1 and Bolts 2 was increased. Also, the RMSD level for the magnetic-mount interface was relatively larger than the level for the glue bonding interface. As shown in Fig. 10(b), for the two steel PZT interfaces (i.e., glue bonding and magnetic bonding interfaces), the RMSD index was went up when increasing the torque-loss in Bolts 1 and Bolts 2. Under the Bolts 2-loosening cases, the RMSD level for the magnetic-mount interface was about half of the RMSD level for the glue bonding interface.

### 3.3.3 Damage quantification by CCD index

The CCD index can be also used as a damage metric index to quantify the change of the impedance signatures measured before and after the damage event (Zagrai and Giurgiutiu 2001).

The CCD index is calculated, as follows

$$CCD = 1 - \frac{1}{\sigma_Z \sigma_Z^*} E\{[Z_i(\omega) - \bar{Z}(\omega)][Z_i^*(\omega) - \bar{Z}^*(\omega)]\} \quad (7)$$

where $E[.]$ is the expectation operation; $\bar{Z}(\omega)$ and $\bar{Z}^*(\omega)$ signify the mean values of impedance signatures before and after the damage; and $\sigma_Z$ and $\sigma_Z^*$ are the standard deviation values of impedance signatures before and after damage.

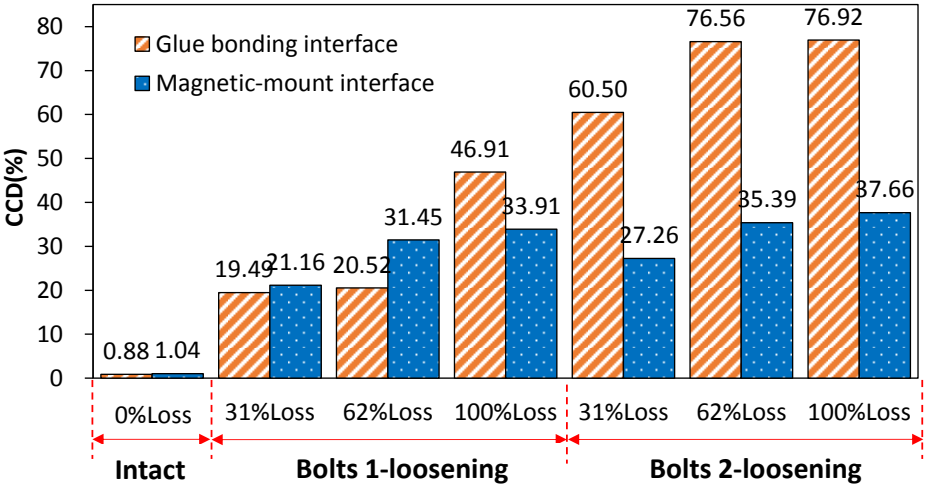


(a) Aluminum PZT interfaces

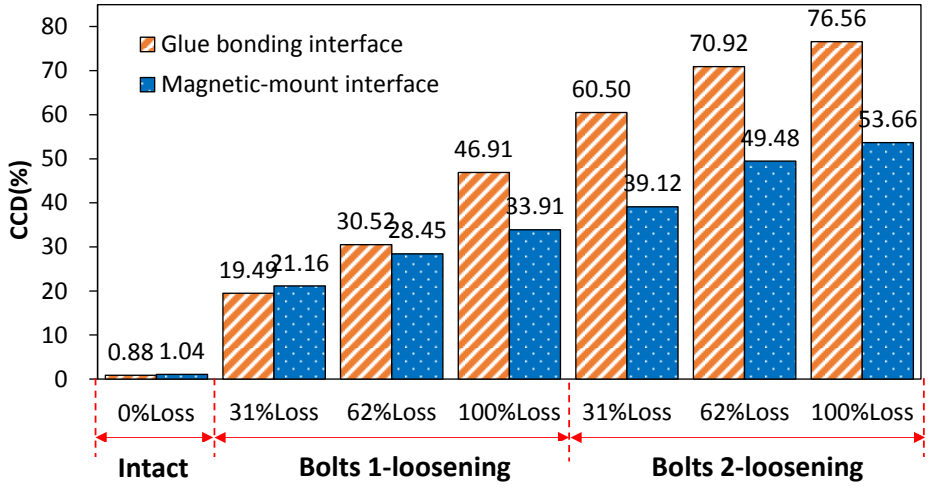


(b) Steel PZT interfaces

Fig. 11 CCD quantification of the bolt-loosening events in steel girder

Fig. 11 shows the damage quantification by CCD with respect to the bolt-loosening events for aluminum and steel PZT interfaces. The CCD index was plotted in a row of torque-loss levels. As shown in Fig. 11(a), for the two aluminum PZT interfaces, the CCD index was increased as the torque-loss in Bolts 1 and Bolts 2 was increased. Under the Bolts 2-loosening events, the CCD level for the magnetic-mount interface was a half of that for the glue bonding interface. As shown in Fig. 11(b), for the two steel PZT interfaces, the CCD index was also went up when increasing the torque-loss in the connection. Under the Bolts 2-loosening events, the CCD level for the magnetic-mount interface was two thirds of the level for the glue bonding interface.

By comparing the two damage indices, it is found that the damage severity of the connection estimated by the CCD index was relatively larger than the estimation by the RMSD index. By comparing the two different materials of interfaces, it is observed that the steel interfaces showed better indication of damage in the bolted connection than the aluminum interfaces in general. The comparison of the two attachment methods revealed that the glue bonding interfaces showed relatively better indication of damage than the magnetic-mount interfaces in general. Despite that, the proposed magnetic-mount PZT interfaces were successful in detecting the bolt-loosening occurrence.

## 4. Conclusions

This study presented an experimental investigation into using magnetically attached PZT-interface for the impedance-based damage detection in bolted girder connections. Firstly, the principle of the impedance-based damage detection method via the PZT-interface device was outlined. Secondly, a PZT-interface attachment method in which permanent magnets were used to replace the conventional epoxy bond was proposed. Finally, the use of the magnetic attraction for the PZT-interface was experimentally evaluated via detecting the bolt-loosening events in a bolted girder connection. Also, the sensitivity of impedance signatures obtained from the PZT-interface was analyzed with regard to the interface's material.

From the experimental investigation, the following concluding remarks can be drawn, as follows:

- The glue bonding method and the magnetic bonding method showed quite consistent impedance signatures at the same frequency ranges and also with identical patterns in general.
- The proposed magnetic-mount PZT interfaces were successful in detecting the bolt-loosening occurrence in the girder connection.
- The damage severity of the connection estimated by the CCD index was relatively larger than that by the RMSD index.
- The steel magnetic-mount interfaces showed better indication of bolt-loosening in the bolted connection than the aluminum magnetic-mount interfaces in general.

However, the glue bonding interfaces showed better indication of bolt-loosening in the bolted connection than the magnetic-mount interfaces. As the future work, more research efforts need to be done on improving the adhesion performance of the magnetic-mount PZT interfaces. Also, the effect of the coating to the connection on the adhesion performance should be investigated.

## Acknowledgments

This work was supported by Basic Science Research Program through the National Research Foundation of Korea (NRF) funded by the Ministry of Education, Science and Technology (NRF 2016R1A2B4015087). The post-doctoral researcher and the graduate student involved in this research were also supported by the Brain Korea 21 Plus program of Korean Government.

## References

Ayres, J.W., Lalande, F., Chaudhry, Z. and Rogers, C.A. (1998), "Qualitative impedance-based health monitoring of civil infrastructures", *Smart Mater. Struct.*, **7**, 599-605.

Giurgiutiu, V. and Zagrai, A. (2005), "Damage detection in thin plates and aerospace structures with the electro-mechanical impedance method", *Struct. Health Monit.*, **4**(2), 99-118.

Ho, D.D., Ngo, T.M. and Kim, J.T. (2014), "Impedance-based damage monitoring of steel column connection: numerical simulation", *Struct. Monit. Maint.*, **1**(3), 339-356.

Huynh, T.C. and Kim, J.T. (2014), "Impedance-based cable force monitoring in tendon-anchorage using portable PZT-interface technique", *Math. Probl. Eng.*, **2014**, 1-11.

Huynh, T.C. and Kim, J.T. (2016), "Compensation of temperature effect on impedance responses of PZT interface for prestress-loss monitoring in PSC girders", *Smart Struct. Syst.*, **17**(6), 881-901.

Huynh, T.C. and Kim, J.T. (2017), "Quantitative damage identification in tendon anchorage via PZT interface-based impedance monitoring technique", *Smart Struct. Syst.*, **20**(2), 181-195.

Huynh, T.C., Lee, K.S. and Kim, J.T. (2015a), "Local dynamic characteristics of PZT impedance interface on tendon anchorage under prestress force variation", *Smart Struct. Syst.*, **15**(2), 375-393.

Huynh, T.C., Park, Y.H., Park, J.H. and Kim, J.T. (2015b), "Feasibility verification of mountable PZT-interface for impedance monitoring in tendon-anchorage", *J. Shock Vib.*, **2015**, 1-11.

Kim, J.T., Huynh, T.C. and Lee, S.Y. (2014), "Wireless structural health monitoring of stay cables under two consecutive typhoons", *Struct.l Monit. Maint.*, **1**(1), 47-67.

Kim, J.T., Park, J.H., Hong, D.S. and Park, W.S. (2010), "Hybrid health monitoring of prestressed concrete girder bridges by sequential vibration-impedance approaches", *Eng. Struct.*, **32**, 115-128.

Kim, J.T., Sim, S.H., Cho, S., Yun, C.B. and Min, JY. (2016), "Recent R&D activities on structural health monitoring in Korea", *Struct. Monit. Maint.*, **3**(1), 91-114.

Li, H.N., Yi, T.H., Ren, L., Li, D.S. and Huo, L.S. (2014), "Review on innovations and applications in structural health monitoring for infrastructures", *Struct. Monit. Maint.*, **1**(1), 1-45.

Li, H.N., Li, D.S., Ren, L., Yi, T.H., Jia, Z.G. and LI, K.P. (2016), "Structural health monitoring of innovative civil engineering structures in Mainland China", *Struct. Monit. Maint.*, **3**(1), 1-32.

Liang, C., Sun, F.P. and Rogers, C.A. (1994), "Coupled electro-mechanical analysis of adaptive material - Determination of the actuator power consumption and system energy transfer", *J. Intel. Mat. Syst. Str.*, **5**, 12-20.

Mascarenas, D, Todd, M.D., Park, G. and Farrar, C.R. (2007), "Development of an impedance-based wireless sensor node for structural health monitoring", *Smart Mater. Struct.*, **16**(6), 2137-2145.

Nagarajaiah, S. and Erazo, K. (2016), "Structural monitoring and identification of civil infrastructure in the United States", *Struct. Monit. Maint.*, **3**(1), 51-69.

Nguyen, K.D. and Kim, J.T. (2012), "Smart PZT-interface for wireless impedance-based prestress-loss monitoring in tendon-anchorage connection", *Smart Struct. Syst.*, **9**(6), 489-504.

Park, G., Sohn, H., Farrar, C. and Inman, D. (2003), "Overview of piezoelectric impedance-based health monitoring and path forward", *Shock Vib. Digest*, **35**(6), 451-463.

Park, J.H., Huynh, T.C. and Kim, J.T. (2015), "Temperature effect on wireless impedance monitoring in tendon anchorage of prestressed concrete girder", *Smart Struct. Syst.*, **15**(4), 1159-1175.

Park, J.H., Kim, J.T., Hong, D.S., Mascarenas, D. and Lynch, J.P. (2010), "Autonomous smart sensor nodes

for global and local damage detection of prestressed concrete bridges based on accelerations and impedance measurements", *Smart Struct. Syst.*, **6**(5), 711-730.

Park, S., Park, G., Yun, C.B. and Farrar, C.R. (2008), "Sensor self-diagnosis using a modified impedance model for active sensing-based structural health monitoring", *Struct. Health Monit.*, doi: 10.1177/1475921708094792.

Soh, C.K., Tseng, K.K., Bhalla, S. and Gupta, A. (2000), "Performance of smart piezoceramic patches in health monitoring of a RC bridge", *Smart Mater. Struct.*, **9**, 533-542.

Sun, F.P., Chaudhry Z., Liang, C. and Rogers C.A. (1995), "Truss structure integrity identification using PZT sensor-actuator", *J. Intel. Mat. Syst. Str.*, **6**, 134-139.

Xu, Y.G. and Liu, G.R. (2002), "A modified electro-mechanical impedance model of piezoelectric actuator-sensors for debonding detection of composite patches", *J. Intel. Mat. Syst. Str.*, **13**, 389-396.

*TY*